

CFD Analysis for Improving Forced Convection Heat Transfer from Newly Designed Perforated Heat Sinks

Ahmed Al-Zahrani

Department of Mechanical and Materials Engineering, Faculty of Engineering, University of Jeddah, Saudi Arabia

aalzahrani@uj.edu.sa (corresponding author)

Received: 27 February 2024 | Revised: 16 March 2024 | Accepted: 20 March 2024

Licensed under a CC-BY 4.0 license | Copyright (c) by the authors | DOI: <https://doi.org/10.48084/etasr.7155>

ABSTRACT

This study develops a 3D-CFD model to analyze the thermal performance of perforated fin heat sinks and evaluates four perforated continuous and interrupted fin heat sinks with distinct geometric patterns. Using the Finite-Volume Method (FVM) to discretize the governing equations, the SolidWorks 2019 flow simulation software was implemented to solve and validate the latter, demonstrating that the CFD simulation model employed in the current study is reliable. The performance parameters of the heat sink are presented in terms of Reynolds number and heater power. The results indicate that modules B and C achieved higher heat transfer rates, average heat transfer coefficient, and Nusselt number compared to the other modules. Module A had the highest fin efficiency and module D exhibited greater fin effectiveness than the other ones.

Keywords-CFD; SolidWorks; forced convection; heat sink

I. INTRODUCTION

Most engineering systems generate heat as they operate. If this heat does not rapidly dissipate into the atmosphere, it could cause the system components to overheat and eventually fail. To prevent this, it is necessary to reject the heat to its surroundings so that the system remains at the desired temperature and continues to function properly [1-3]. To increase surface heat transfer, expanded surfaces (fins) are used in several applications. It is common for fin materials to have high thermal conductivity, which allows for the heat transfer from a wall to the fin when the latter is subjected to a flowing fluid, which can either heat or cool it. In addition to their contribution to improving convective heat transfer, fins provide significant methods for increasing total heat transfer surface area while minimizing the use of the primary surface area, which is beneficial in many engineering applications [4].

Fins are also frequently deployed in power management, electrical, and automotive systems. They function as heat sinks, dissipating excess heat from moving or processing systems or mechanisms [5-7], such as engine cooling or condensers in air conditioning and refrigeration [8-10]. In addition, fins are utilized in gas turbine blade trailing edges, the aerospace sector, and electronic cooling. Relative fin height (H/d) affects the heat transfer of pins to pins [5]. Installing a fin on the surface or an extended surface can typically significantly boost the heat transfer rate in cases where the convective heat transfer coefficient is minimal, which is primarily encountered when the surrounding fluid is gas. Furthermore, straight fins, spines,

pin fins, and circumferential or annular fins may also be considered forms of expanded surface [11]. Additionally, pin fins have several industrial applications due to their high heat transfer efficiency, including cooling electronics, heat exchangers, gas turbine blades, and more [12]. Perforated fins increase heat transfer and reduce material weight [13]. Fin spacing and shape affect heat transmission [14-16]. The ideal perforation shape for better heat transfer is unknown. According to [4], increasing the heat transfer coefficient or the fin surface area improves the heat transfer. Many studies have investigated how to increase the heat transfer of fins. In [17], the effect of perforation on heat transfer was studied in modern thermal systems, disclosing that the heat coefficient increases the heat transfer rate.

Recent studies have improved compact, lightweight designs to maximize heat dissipation with little material exposure, including choosing material, perforated, and interrupted plates [18-19]. Some studies add cavities, holes, slots, grooves, or channels to fin bodies to increase the heat transfer area and coefficient. Perforated studies help to raise the heat transfer coefficient. The surface of heat transmission is augmented by perforating the fin bodies [13]. In [20], mixed convection in a 3D square duct with different fin configurations was statistically evaluated in laminar and turbulent flows. Inclined fins promote heat transfer by 40-50% under laminar flow conditions and 15-20% in turbulent flow over base plate heat transfer. The effect of limiting heat input on temperature distribution has been extensively studied. The fin temperature dramatically drops when the fins are optimally arranged in the

air flow stream. In [21], an innovative Plate-Pin Fin (PPF) heat sink was numerically and experimentally investigated. A straightforward plate-fin heat sink was altered by spacing several column-shaped pins between the plate fins. Under the same conditions, it was discovered that PPF had 30% less thermal resistance than plate-fin heat sinks. In [22], the thermal performance and the convective heat transfer coefficient of plate fins and plate cubic pin-fin heat sinks were explored under natural convection. Compared to plate-fin heat sinks, plate-cube pin-fins were more effective heat transfer agents with a remarkable improvement of 10-41.6%.

Plate-fin heat sinks are the most popular ones because of their simple shape and satisfactory thermal performance. This study investigates a new interrupted perforated plate with cubic pin-fin heat sinks, continuous and interrupted plate-fin heat sinks, and cubical pins with linear arrangements between plate fins. Four different modules, namely perforated plate fin-tilted square pin fin (Module A), inclined perforated plate conv div-tilted square pin fin (Module B), corrugated perforated plate-tilted square pin fin (Module C), and inclined perforated parallel plate-tilted square pin fin model (Module D) are presented and evaluated. The heat transfer enhancement for modules with different heat sink powers and Reynolds numbers was studied and compared using 3D-CFD.

II. CFD MODELING AND ANALYSIS

A. Problem Description

Holes are punched into the fins to prevent the viscous boundary layer from expanding along the plain fins. Furthermore, the fins are improved with perforations, which are circular holes, to provide a better rate of heat transfer and reduce temperature. Four heat sink modules were examined in this study using forced convection:

- Module A: Perforated plate fin-tilted square pin fin.
- Module B: Inclined perforated plate conv div-tilted square pin fin.
- Module C: Corrugated perforated plate-tilted square pin fin.
- Module D: Inclined perforated parallel plate-tilted square pin fin.

In the simulation, each heat sink is studied at power supply values of 20, 40, 60, 80, and 100W, and different values of air inlet velocity of 0.5, 0.75, 1, 1.25, 1.5, 1.75, and 2 m/s. During simulation, the air inlet temperature is maintained at 22°C to simulate an air conditioning environment, which varies from 22 to 25°C to achieve thermal comfort conditions. All heat sinks are aluminum alloy with 239 W/m.K thermal conductivity. Figure 1 depicts the CAD models of the proposed heat sinks with detailed dimensions.

B. Numerical Methodology and Validation

The computational domains for the rectangular wind channel with a constant heat flux at the base of the heat sink are demonstrated in Figure 2. Furthermore, in conjunction with an atmospheric temperature of 22°C, uniform velocity at the input and no-slip boundary conditions at the exit are implemented.

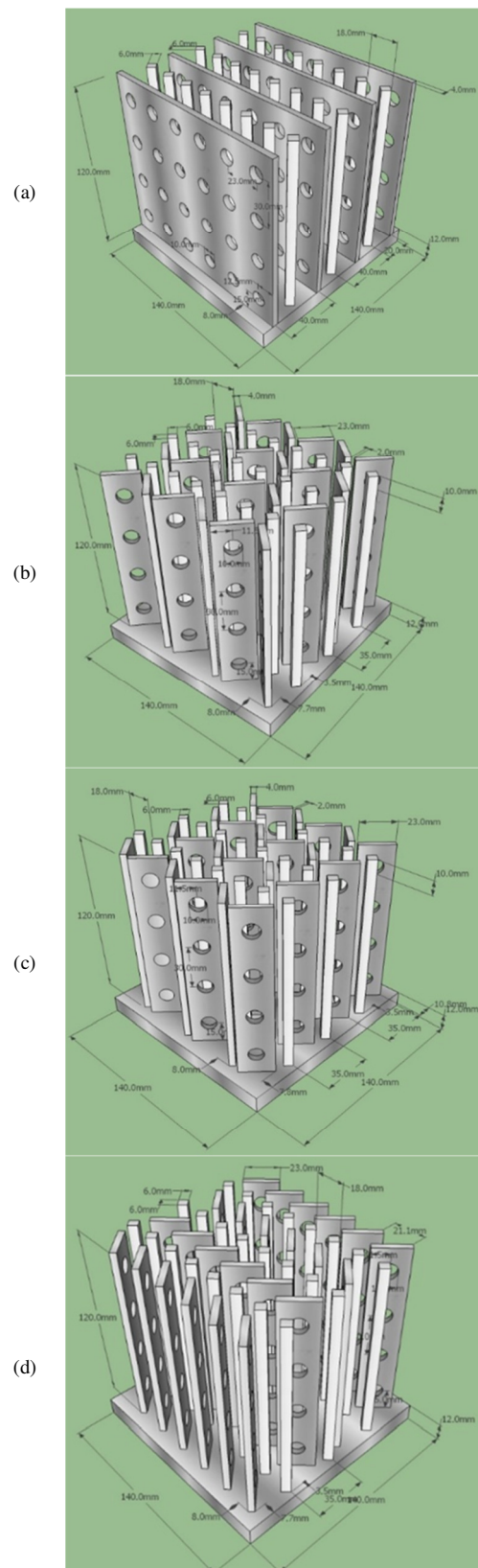


Fig. 1. CAD models of the proposed heat sinks: (a) Module A, (b) Module B, (c) Module C, (d) Module D.

The thermal insulation of the exterior walls of the rectangular flow channel was proposed. Simulations were carried out using the SolidWorks 2019 flow simulation software. To confirm the solution's independence from grid size, extensive numerical testing is conducted on each module. This verification process involves comparing the Nusselt numbers and the average temperature associated with the heat sinks. Furthermore, to ensure adequate resolution, a quadratic mesh grid consisting of 2,425 edge elements, 51,322 boundary elements, and 149,063 domain elements was implemented. The coupled system of equations was solved through an iterative process. A solution is considered to have converged when the relative error between two subsequent iterations in each of the fields is less than 1.0×10^{-6} [23-24]. To validate the Computational Fluid Dynamics (CFD) results of this study, the Nusselt number of smooth plates without fins was compared with experimental data, as illustrated in Figure 3. The agreement between the experimental and CFD results indicates that the CFD simulation model used is reliable.

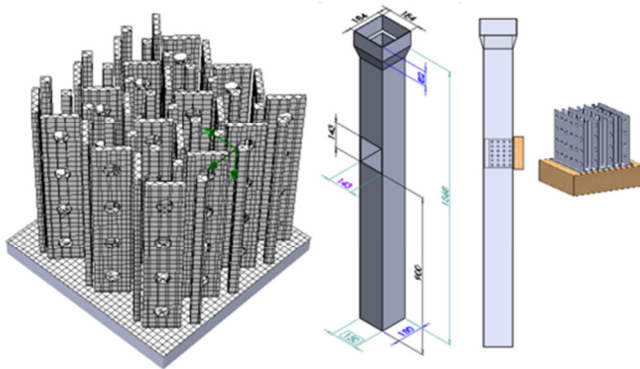


Fig. 2. 3D computational domain: (a) module meshing, (b) wind tunnel (dimensions in mm).

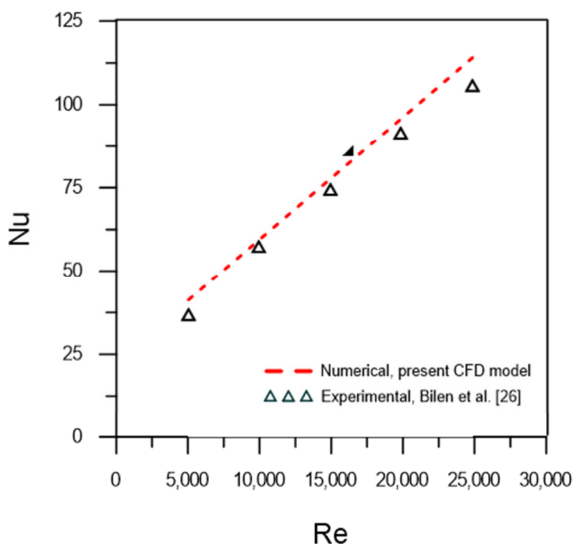


Fig. 3. Comparison of the Nusselt numbers obtained experimentally by [26] and the current CFD model for a flat plate free of fins.

C. Governing Equations

SolidWorks 2019 Flow Simulation deploys established CFD technology to calculate fluid (gas or liquid) flows, inside and outside SolidWorks models, and heat transfer due to convection, radiation, and conduction [26-27]. SolidWorks 2019 flow simulation employs transport equations for dissipation rate and turbulent kinetic energy utilizing a $k-\epsilon$ model. The flow conditions are predicted using the Navier-Stokes equations. The damping function of the modified $k-\epsilon$ model, as presented in [28], provides a mathematical framework for characterizing fluid flow behavior. The concepts of fluid dynamics' turbulence conservation are applied in this model. Its primary strength is its ability to accurately depict the intricate relationships between fluid motion and turbulence.

$$\frac{\partial}{\partial t}(\rho k) + \frac{\partial}{\partial x_i}(\rho k u_i) = \frac{\partial}{\partial x_i} \left[\left(\mu + \frac{\mu_t}{\sigma_k} \right) \frac{\partial k}{\partial x_j} \right] + \tau_{ij}^R \frac{\partial u_i}{\partial x_j} - \rho \epsilon + \mu_t P_B \quad (1)$$

$$\frac{\partial}{\partial t}(\rho \epsilon) + \frac{\partial}{\partial x_i}(\rho \epsilon u_i) = \frac{\partial}{\partial x_i} \left[\left(\mu + \frac{\mu_t}{\sigma_\epsilon} \right) \frac{\partial \epsilon}{\partial x_j} \right] + C_{\epsilon 1} \frac{\epsilon}{\kappa} \left(f_1 \tau_{ij}^R \frac{\partial u_i}{\partial x_j} + C_B \mu_t P_B \right) - f_2 C_{\epsilon 2} \frac{\rho \epsilon^2}{\kappa} \quad (2)$$

$$\tau_{ij} = \mu S_{ij}, \tau_{ij}^R = \mu_t S_{ij} - \frac{2}{3} \rho \kappa \delta_{ij}, \quad S_{ij} = \frac{\partial u_i}{\partial x_j} + \frac{\partial u_j}{\partial x_i} - \frac{2}{3} \delta_{ij} \frac{\partial u_\kappa}{\partial x_\kappa} \quad (3)$$

$$P_B = \frac{g_i}{\sigma_B} \frac{1}{\rho} \frac{\partial \rho}{\partial x_i} \quad (4)$$

where $C_\mu = 0.09$, $C_{\epsilon 1} = 1.44$, $C_{\epsilon 2} = 1.92$, $\sigma_k = 1$, $\sigma_\epsilon = 1.3$, $\sigma_B = 0.9$, and $C_B = 1$ if $P_B > 0$.

Turbulent viscosity is calculated as:

$$\mu_t = f_\mu \times \frac{C_\mu \rho \kappa^2}{\epsilon} \quad (5)$$

The dumping function calculation is defined as [28]:

$$f_\mu = (1 - e^{-0.025 R_y})^2 \times \left(1 + \frac{20.5}{R_t} \right) \quad (6)$$

where:

$$R_y = \frac{\rho \sqrt{\kappa y}}{\mu} \quad (7)$$

$$R_t = \frac{\rho \kappa^2}{\mu \epsilon} \quad (8)$$

D. Data Analysis

The average heat transfer between the heat sink surface temperature and the average mean air temperature can be calculated as:

$$h = \frac{Q}{A_s [t_s - t_{mean}]} \quad (9)$$

The average Nussult number based on hydraulic duct diameter and average heat transfer coefficient is determined by:

$$Nu = \frac{hD_h}{k_{air}t_{mean}} \quad (10)$$

Fin efficiency is the ratio of the actual heat transfer to the maximum value of the heat sink and is calculated by:

$$\eta_{fin} = \frac{Q}{Q_{max}}, \quad Q_{max} = hA_s(t_b - t_{mean}) \quad (11)$$

where $\eta_{fin} < 1$. Fin effectiveness is the ratio of the actual heat transfer rate to the heat rate based on the heat sink temperature base and is calculated by:

$$\varepsilon_{fin} = \frac{Q}{hA_b(t_b - t_{mean})} = \frac{A_s}{A_b} \eta_{fin} \quad (12)$$

where $\varepsilon_{fin} > 1$.

III. RESULTS AND DISCUSSION

The thermal performance of the new design of four perforated plate-fin heat sink modules (modules A, B, C, and D) was numerically studied under forced convection conditions. Exploring the CFD of a new design for a heat sink is crucial for the thermal management and cooling of electronic devices. As electronic components decrease in size and grow in power density, efficient heat dissipation becomes crucial for maintaining peak performance and reliability. The design of the perforated plate fin has unique characteristics that can greatly influence thermal performance, including an increased surface area and increased airflow. CFD models are used to examine the heat transfer properties, fluid flow patterns, and temperature distribution inside the heat sink. This comprehensive approach enables iterative improvement of the design, maximizing its efficiency in dispersing heat. The effect of the operating parameters, namely the Reynolds number (Re) from 5,000 to 20,000 and the heater power (Q) from 20 to 100 W, on thermal performance, entailing heat sink surface temperature distribution, convection heat transfer coefficient (h), Nusselt number (Nu), fin efficiency (η_f), and fin effectiveness (ε_f), was investigated for the four proposed heat sink modules.

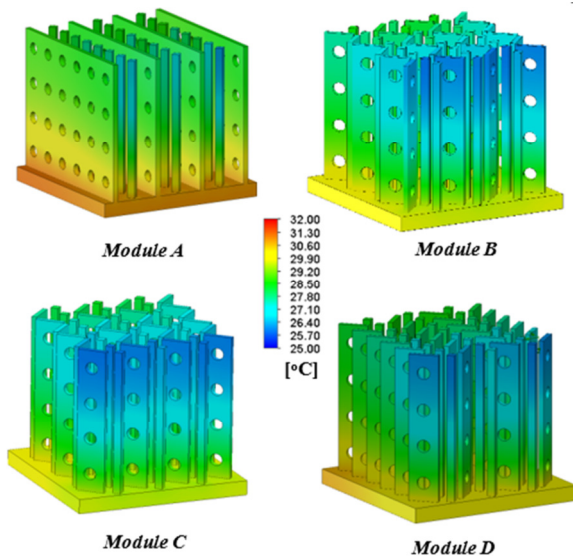


Fig. 4. Surface temperature distributions of modules A, B, C, and D at $Re = 5000$ and $Q = 20$ W.

The numerical simulations were performed with various Reynolds numbers (5,000-20,000) and heater power (20-100 W). The simulations were carried out under steady-state conditions, which is also a crucial aspect. Figures 4 and 5 exhibit contour maps that depict the surface temperature distributions of the heat sink modules examined at Reynolds numbers of 5,000 and 20,000, respectively, and $Q = 20$ W. These figures indicate that increasing the vortices inside the heat sink by controlling and directing the fluid at the entrance of the heat sink and consequently increasing recirculation zones and velocity fluctuations in proximity to the walls leads to improved heat transfer efficiency.

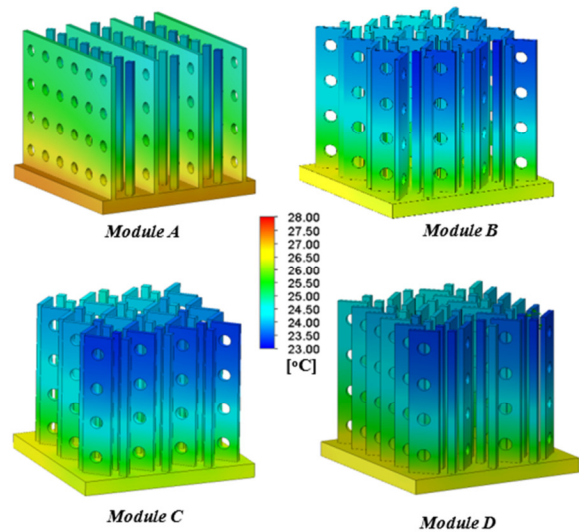


Fig. 5. Surface temperature distributions of modules A, B, C, and D at $Re = 20000$ and $Q = 20$ W.

However, this improvement may not be consistent when considering other physical phenomena, such as the heat sink surface area. With increasing Re , the surface temperatures of all modules decrease, especially for modules B and C. Also, the maximum surface temperature occurs at the heated base wall of the heat sink. The figures clearly show that there was a notable increase in heat dissipation in modules B and C compared to modules A and D, attributable to variations in the inclined perforated conversion-diversion V tilted square pin fin in module B, the inclined perforated parallel plate tilted square pin fin in module C, and the flow directional aspects within each module. This highlights the positive influence of turbulence generated by the perforated conversion diversion and parallel plate on the fundamental heat transfer performance at the module's surface.

Figure 6 displays the effect of heater power ($Q = 20$ W and $Q = 100$ W) on the surface temperature distributions of module A at $Re = 5000$. Figures 7 and 8 depict the average heat transfer coefficient (h) and Nu for all heat sink modules at various Reynolds numbers and specified heater power (Q). Figure 7 reveals that the heater power does not affect the average convective heat transfer coefficient. This can be attributed to the heat transfer coefficient calculated based on the heat flux and the temperature difference between the average

temperature of the heat sink surface and the average air temperature at the inlet and outlet from the heat sink, where with increasing heater power the temperature difference rises. Furthermore, Figures 7 and 8 demonstrate that the heat transfer coefficient and Nu increase with increasing Reynolds number, and it is also clear that modules B and C have higher heat transfer coefficients than A and D due to increasing flow turbulence that results in improved transport rates.

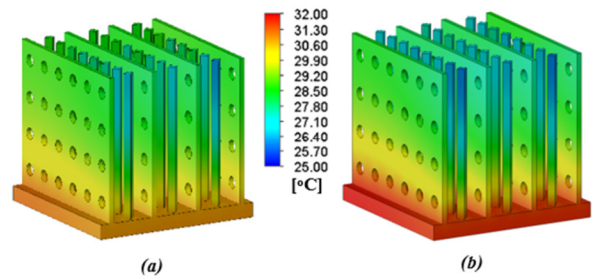


Fig. 6. Surface temperature distributions of module A at $Re = 5000$: (a) $Q = 20$ W, (b) $Q = 100$ W.

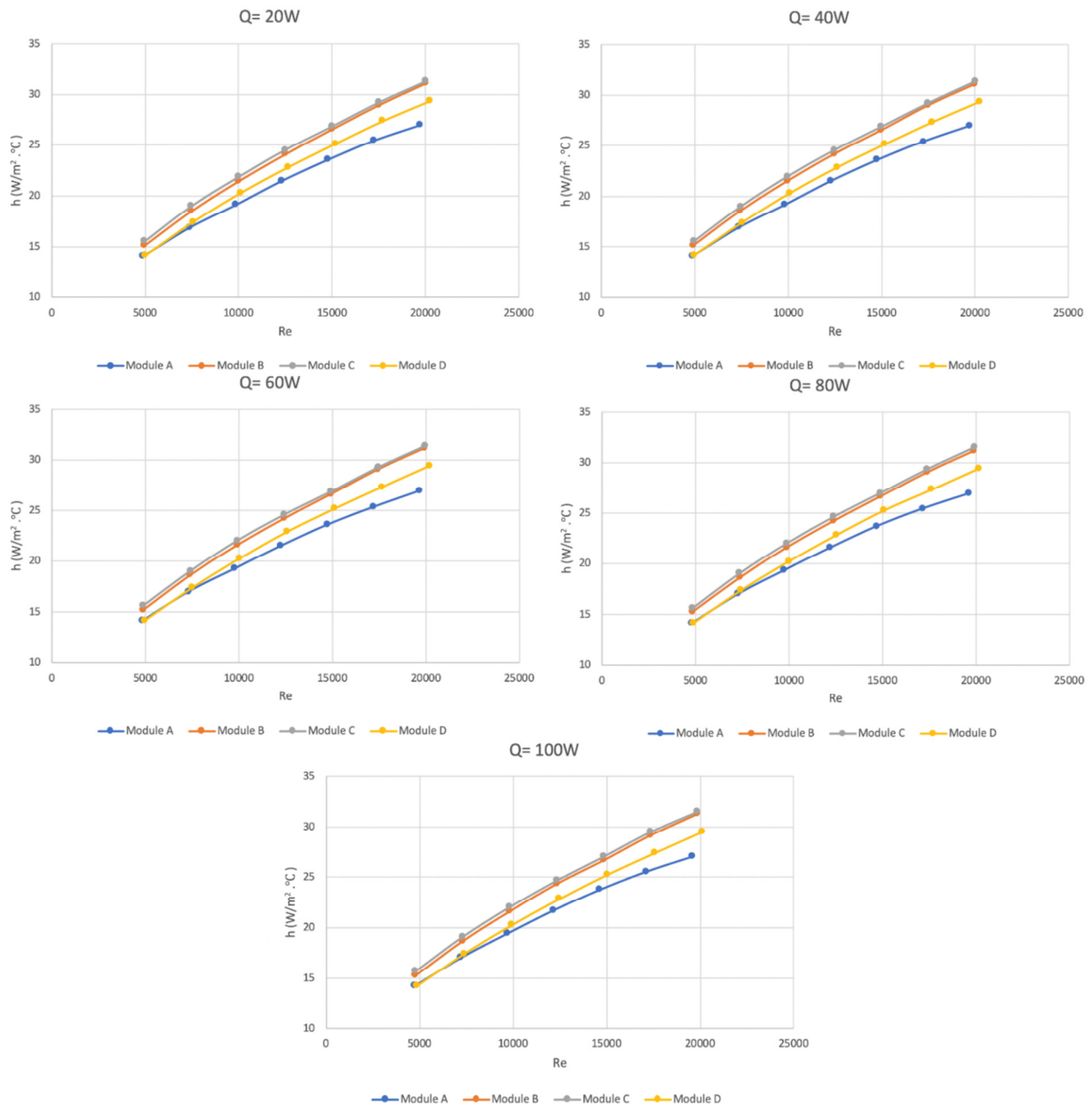


Fig. 7. Effect of Reynolds number on the average heat transfer coefficient for modules A, B, C, and D for different heater power.

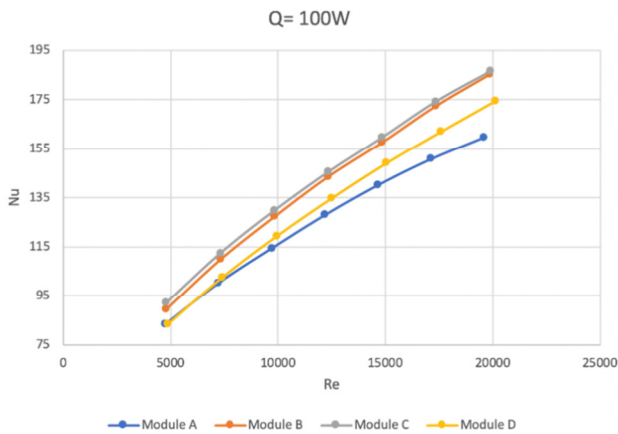


Fig. 8. Effect of Reynolds number on the average Nusselt number for modules A, B, C, and D at Q= 100 W.

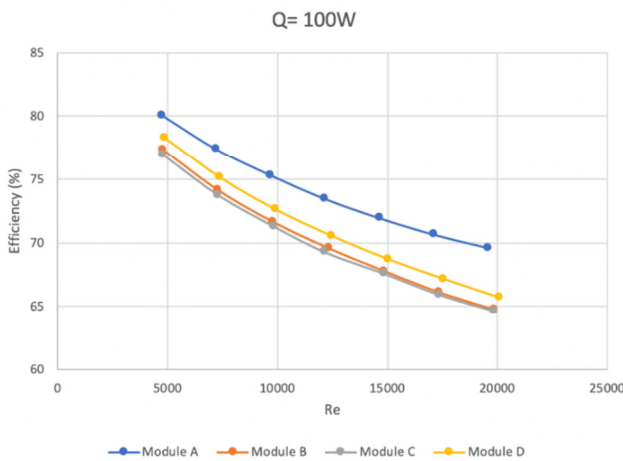


Fig. 9. Effect of Reynolds number on the fin efficiency (η_f) for modules A, B, C, and D at Q= 100 W.

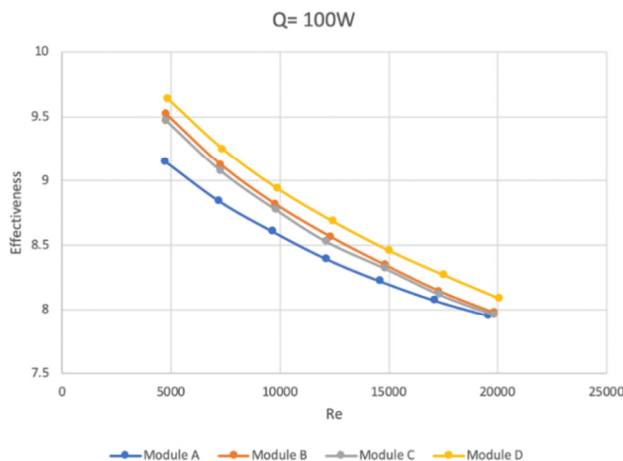


Fig. 10. Effects of Reynolds number on the fin effectiveness (ϵ_f) for modules A, B, C, and D at Q= 100 W.

Figures 9 and 10 illustrate the impact of the Reynolds number on fin efficiency (η_f) and fin effectiveness (ϵ_f) across

various types of perforated heat sink modules. Figure 9 indicates that module A exhibits a relatively higher fin efficiency compared to modules B, C, and D. The trend reveals a decline in fin efficiency as the Reynolds number increases. This decrease is attributed to the observed reduction in the base temperature of the heat sink at higher flow rates, as observed in Figure 9. On the other hand, Figure 10 shows that module D exhibits the highest effectiveness, followed by modules B and C, while module A had a lower fin effectiveness (η_f).

IV. CONCLUSIONS

A CFD model was developed to analyze the thermal performance, namely heat sink surface temperature distribution, convection heat transfer coefficient h , Nusselt number, fin efficiency (η_f), and fin effectiveness (ϵ_f), of four perforated plate-fin heat sink modules using the SolidWorks 2019 flow simulation software. This study demonstrated the performance parameters of the heat sink as a function of Reynolds number and heater power. The results indicated that modules B, and C achieved higher heat transfer rate, average heat transfer coefficient, and Nusselt number than modules A and D. Moreover, the fin efficiency (η_f) was higher for module A than for modules B, C, and D, and module D exhibited higher fin effectiveness (ϵ_f) compared to the other modules. The average Nusselt number for modules B and C was 6% and 18% higher compared to modules D and A, respectively. The average Nusselt number for modules B and C increased by 105%, and the fin effectiveness (ϵ_f) of module D decreased by 15.6 with an augmentation in Reynolds number from 5000 to 20000. Future work may consider the effects of pressure drop and thermal-hydraulic performance factor.

NOMENCLATURE

A_s	The surface area of the heat sink, m^2
A_b	Surface area of heat sink base, m^2
D_h	Hydraulic diameter, m
h	Average heat transfer coefficient, $W/m^2 \cdot ^\circ C$
K_{air}	Average thermal conductivity of air, $W/m \cdot ^\circ C$
Nu	Average Nusselt number
Q	Convective heat transfer, W
Q_{max}	Power of heater, W
Re	Reynolds number
t_s	The average surface temperature of the heat sink, $^\circ C$
t_{mean}	The average temperature of the air, $^\circ C$
v	Air velocity, m/s
Greek symbols	
μ	Air dynamic Viscosity, $kg/m \cdot s$
ν	Air kinematic viscosity, m^2/s
η_{fin}	Fin efficiency
ϵ_{fin}	Fin effectiveness

REFERENCES

[1] A. A. Walunj and D. D. Palande, "Experimental analysis of inclined narrow plate-fins heat sink under natural convection," *IPASJ*

- International Journal of Mechanical Engineering*, vol. 2, no. 6, pp. 8–13, Jun. 2014.
- [2] K. Boukerma and M. Kadja, "Convective Heat Transfer of Al₂O₃ and CuO Nanofluids Using Various Mixtures of Water-Ethylene Glycol as Base Fluids," *Engineering, Technology & Applied Science Research*, vol. 7, no. 2, pp. 1496–1503, Apr. 2017, <https://doi.org/10.48084/etasr.1051>.
- [3] E. C. Romao and L. H. P. de Assis, "Numerical Simulation of 1D Unsteady Heat Conduction-Convection in Spherical and Cylindrical Coordinates by Fourth-Order FDM," *Engineering, Technology & Applied Science Research*, vol. 8, no. 1, pp. 2389–2392, Feb. 2018, <https://doi.org/10.48084/etasr.1724>.
- [4] R. R. Jassem, "Effect the form of perforation on the heat transfer in the perforated fins," *Academic Research International*, vol. 4, no. 3, pp. 198–207, 2013.
- [5] A. B. Dhumne and H. S. Farkade, "Heat transfer analysis of cylindrical perforated fins in staggered arrangement," *International Journal of Innovative Technology and Exploring Engineering*, vol. 2, no. 5, pp. 225–230, 2013.
- [6] A. A. Bhuiyan and A. K. M. S. Islam, "Thermal and hydraulic performance of finned-tube heat exchangers under different flow ranges: A review on modeling and experiment," *International Journal of Heat and Mass Transfer*, vol. 101, pp. 38–59, Oct. 2016, <https://doi.org/10.1016/j.ijheatmasstransfer.2016.05.022>.
- [7] R. Rosli, K. A. M. Annuar, and F. S. Ismail, "Optimal Pin Fin Heat sink Arrangement for Solving Thermal Distribution Problem," *Journal of Advanced Research in Fluid Mechanics and Thermal Sciences*, vol. 11, no. 1, pp. 1–18, 2015.
- [8] S. Singh, K. Sørensen, and T. J. Condra, "Influence of the degree of thermal contact in fin and tube heat exchanger: A numerical analysis," *Applied Thermal Engineering*, vol. 107, pp. 612–624, Aug. 2016, <https://doi.org/10.1016/j.applthermaleng.2016.07.022>.
- [9] D. Sahel, H. Ameer, R. Benzeguir, and Y. Kamla, "Enhancement of heat transfer in a rectangular channel with perforated baffles," *Applied Thermal Engineering*, vol. 101, pp. 156–164, May 2016, <https://doi.org/10.1016/j.applthermaleng.2016.02.136>.
- [10] R. V. Dhanadhya, A. S. Nilawar, and Y. L. Yenarkar, "Theoretical study and finite element analysis of convective heat transfer augmentation from horizontal rectangular fin with circular perforation," *International Journal of Mechanical and Production Engineering Research and Development*, vol. 3, no. 2, pp. 187–192, Jun. 2013.
- [11] H. Nabati, "Optimal Pin Fin Heat Exchanger Surface," Ph.D. dissertation, Mälardalen University, Sweden, 2008.
- [12] S. D. Bahadure and G. D. Gosavi, "Enhancement of Natural Convection Heat Transfer from Perforated Fin," *International Journal of Engineering Research*, vol. 3, no. 9, pp. 531–535, 2014.
- [13] Md. F. Ismail, M. N. Hasan, and M. Ali, "Numerical simulation of turbulent heat transfer from perforated plate-fin heat sinks," *Heat and Mass Transfer*, vol. 50, no. 4, pp. 509–519, Apr. 2014, <https://doi.org/10.1007/s00231-013-1242-8>.
- [14] M. Zhou, Y. He, and Y. Chen, "A heat transfer numerical model for thermoelectric generator with cylindrical shell and straight fins under steady-state conditions," *Applied Thermal Engineering*, vol. 68, no. 1, pp. 80–91, Jul. 2014, <https://doi.org/10.1016/j.applthermaleng.2014.04.018>.
- [15] C. H. Huang and Y. L. Chung, "A nonlinear fin design problem in determining the optimum shapes of fully wet annular fins," *Applied Thermal Engineering*, vol. 103, pp. 195–204, Jun. 2016, <https://doi.org/10.1016/j.applthermaleng.2016.03.066>.
- [16] G. A. Chaudhari, I. N. Wankhede, and M. H. Patil, "Effect of Percentage of Perforation on the Natural Convection Heat Transfer from a Fin Array," *International Journal of Engineering and Technical Research*, vol. 3, no. 2, pp. 65–69, Feb. 2015.
- [17] M. R. Shaeri, M. Yaghoubi, and K. Jafarpur, "Heat transfer analysis of lateral perforated fin heat sinks," *Applied Energy*, vol. 86, no. 10, pp. 2019–2029, Oct. 2009, <https://doi.org/10.1016/j.apenergy.2008.12.029>.
- [18] A. Bar-Cohen, M. Iyengar, and A. D. Kraus, "Design of Optimum Plate-Fin Natural Convective Heat Sinks," *Journal of Electronic Packaging*, vol. 125, no. 2, pp. 208–216, Jun. 2003, <https://doi.org/10.1115/1.1568361>.
- [19] R. B. Gurav, J. D. Patil, S. M. Gaikwad, P. Purohit, and A. A. Ramgude, "Finite volume analysis of convective heat transfer augmentation from horizontal rectangular fin by elliptical perforations," *International Journal of Global Technology Initiatives*, vol. 2, no. 1, Mar. 2013.
- [20] M. Mokhtari, M. Barzegar Gerdroodbary, R. Yeganeh, and K. Fallah, "Numerical study of mixed convection heat transfer of various fin arrangements in a horizontal channel," *Engineering Science and Technology, an International Journal*, vol. 20, no. 3, pp. 1106–1114, Jun. 2017, <https://doi.org/10.1016/j.jestech.2016.12.007>.
- [21] X. Yu, J. Feng, Q. Feng, and Q. Wang, "Development of a plate-pin fin heat sink and its performance comparisons with a plate fin heat sink," *Applied Thermal Engineering*, vol. 25, no. 2, pp. 173–182, Feb. 2005, <https://doi.org/10.1016/j.applthermaleng.2004.06.016>.
- [22] S. S. Haghghi, H. R. Goshayeshi, and M. R. Safaei, "Natural convection heat transfer enhancement in new designs of plate-fin based heat sinks," *International Journal of Heat and Mass Transfer*, vol. 125, pp. 640–647, Oct. 2018, <https://doi.org/10.1016/j.ijheatmasstransfer.2018.04.122>.
- [23] H. A. Alhattab, M. A. Albaghdadi, R. S. Hashim, and A. H. Ali, "Design of micro heat sink for power transistor by using CFD," in *2016 Al-Sadeq International Conference on Multidisciplinary in IT and Communication Science and Applications (AIC-MITCSA)*, Baghdad, Iraq, May 2016, <https://doi.org/10.1109/AIC-MITCSA.2016.7759948>.
- [24] M. A. R. Sadiq Al-Baghdadi, Z. M. H. Noor, A. Zeiny, A. Burns, and D. Wen, "CFD analysis of a nanofluid-based microchannel heat sink," *Thermal Science and Engineering Progress*, vol. 20, Dec. 2020, Art. no. 100685, <https://doi.org/10.1016/j.tsep.2020.100685>.
- [25] K. Bilen, U. Akyol, and S. Yapici, "Heat transfer and friction correlations and thermal performance analysis for a finned surface," *Energy Conversion and Management*, vol. 42, no. 9, pp. 1071–1083, Jun. 2001, [https://doi.org/10.1016/S0196-8904\(00\)00119-9](https://doi.org/10.1016/S0196-8904(00)00119-9).
- [26] F. A. Alnaimat, "The Geometrical Effect on the Von Mises Stress on Ball and Socket Artificial Discs," *Engineering, Technology & Applied Science Research*, vol. 10, no. 5, pp. 6330–6334, Oct. 2020, <https://doi.org/10.48084/etasr.3789>.
- [27] M. Stan and D. G. Zisopol, "Modeling and Optimization of Piston Pumps for Drilling," *Engineering, Technology & Applied Science Research*, vol. 13, no. 2, pp. 10505–10510, Apr. 2023, <https://doi.org/10.48084/etasr.5714>.
- [28] C. K. G. Lam and K. Bremhorst, "A Modified Form of the k-ε Model for Predicting Wall Turbulence," *Journal of Fluids Engineering*, vol. 103, no. 3, pp. 456–460, Sep. 1981, <https://doi.org/10.1115/1.3240815>.

AUTHORS PROFILE

Ahmed Al-Zahrani is an Associate Professor in the Department of Mechanical and Materials Engineering, Faculty of Engineering, University of Jeddah, Saudi Arabia. He received his Ph.D. in Mechanical Engineering from the Department of Mechanical Engineering, Engineering Faculty, Tsinghua University, Beijing, China. His research interests include manufacturing processes, refrigeration and air conditioning, ultra-precision cutting FEM, and renewable energy.